

Fine Structure of the band edge Excitons and Trions in CdSe/CdS Core/Shell Nanocrystals.

A. Shabaev

George Mason University, Fairfax VA 22030, USA

A. V. Rodina

Ioffe Physical-Technical Institute RAS, 194021 St.-Petersburg, Russia

Al. L. Efros

Naval Research Laboratory, Washington DC 20375, USA

Abstract

We present a theoretical description of excitons and positively and negatively charged trions in "giant" CdSe/CdS core-shell nanocrystals (NCs). The developed theory provides the parameters describing the fine structure of excitons in CdSe/CdS core/thick shell NCs as a function of the CdSe/CdS conduction band offset and the CdSe core radius. We have also developed a general theory describing the fine structure of positively charged trions created in semiconductor NCs with a degenerate valence band. The calculations take into account the complex structure of the CdSe valence band and inter-particle Coulomb and exchange interaction. Presented in this paper are the CdSe core size and CdSe/CdS conduction band offset dependences (i) of the positively charged trion fine structure, (ii) of the binding energy of the negatively charged trion, and (iii) of the radiative decay time for excitons and trions. The results of theoretical calculations are in qualitative agreement with available experimental data.

PACS numbers: 73.22.-f, 78.67.Bf, 81.05.Dz

I. INTRODUCTION

Growing attention to CdSe/CdS core/thick shell nanocrystals (NCs) initially reported by two groups^{1,2} is stimulated by their superior optical properties superior to any other NC hetero-structures prepared up to now. The photoluminescence is never completely quenched in these NCs³ and the blinking is almost completely suppressed^{1,4}. At low temperatures these structures demonstrate suppression of non-radiative Auger recombination⁵ and almost 100% photoluminescence quantum yield⁶. As a result these NC structures demonstrate a very low threshold for optically pumped lasing⁷.

The origin of such outstanding optical properties of the CdSe/CdS core/thick shell nano-structures (or giant CdSe/CdS NCs²) is not completely understood, but one thing is clear. The very thick shell always prevents carrier escape to the NC, no matter which mechanism is responsible for this escape: direct quantum mechanical tunneling, thermo-ionization of the NCs, or Auger auto-ionization of the NCs, where two electron hole pairs were created simultaneously⁸. The prevention of the NC ionization could explain the blinking suppression; however, it does not explain the suppression of non-radiative Auger recombination of charged excitons, biexcitons^{1,4,6,9} and multi-excitons^{5,10}.

The alloying of the CdSe/CdS interface in giant CdSe/CdS NCs could be a reason for Auger recombination suppression, as was suggested in several papers of the Los Alamos group^{5-7,10}. This explanation relies on a theoretical prediction that softening of the carrier confined potential could reduce the Auger recombination rate by three orders of magnitude^{11,12}. Indeed, growth of the thick shell in the giant CdSe/CdS core/shell NCs lasted for a week^{5-7,10}. The slow growth of the shell at temperatures above room temperature suggests that the strong interface diffusion takes place during the NC growth. The diffusion should lead to alloying adjacent to the surface area and softening of the confinement potential. This alloying assumption was confirmed recently by the demonstration of mixed phonon replicas in the fluorescence line narrowing (FLN) of CdSe/CdS NCs with a thick shell¹⁰.

This argument, however, cannot be used to explain the suppression of the Auger recombination observed by Dubertret group^{1,3}. The shell of their NCs is grown very fast and that practically excludes any inter-diffusion. In contrast, the fast growth of the lattice mismatched CdSe/CdS core/shell NCs should obviously results in some intrinsic strains.

Indeed, the samples exhibit a phonon spectrum of a pure CdSe NC, the frequencies of which are shifted from bulk CdSe frequencies due to the compressive strain within the NC¹³.

An understanding of the unusual and potentially useful properties of the giant CdSe/CdS core/shell NCs requires a theoretical description of the fine structure of the band edge excitons, and trions. Up to now, the energy spectra of these NC quantum dots were studied only within simplified parabolic band models^{10,14,15}, which do not take into account the complex structure of the valence band and the complicated character of inter-particle Coulomb interactions. The theoretical description of the energy spectra of the exciton and exciton complexes in these NCs also has some objective complications, because CdSe/CdS heterostructures are not well characterized. We know that holes are always localized in CdSe, and that the valence band offset is no less than 500 meV. However, we don't know the sign of the band-offset of the conduction band nor its magnitude. A small value of the CdSe/CdS conduction band offset suggests its complex behavior, because the band offset sign and magnitude should be sensitive to the strain and temperature¹⁴.

These qualitative data on the band offset suggest that an exciton created in CdSe/CdS NCs with a thick CdS shell should look like a donor center, where a hole is strongly localized in the CdSe core while an electron is attracted to this charged core by the Coulomb potential. If CdSe/CdS is the type II hetero-structure, the core potential in the NC pushes the electron into the CdS shell. In the opposite case, if CdSe/CdS is the type I heterostructure, the core creates an additional well, which increases the electron localization around the hole. The temperature dependence of the CdSe and CdS energy gaps¹⁶ suggests that a decrease of temperature should favor type I. As a result, a decrease of the temperature increases the exciton binding energy and, consequently, shortens the radiative decay time of excitons, which is controlled by the electron-hole wave function overlap, and increases the dark-bright exciton splitting.¹⁴

Due to the very strong confinement of holes, the positively charged trion which was observed in the CdSe/CdS NCs⁴ appears as a doubly-charged donor. The larger Coulomb attraction of the electron to the core should significantly increase the electron binding energy and shorten the radiative decay time. The negatively charged exciton should look like a negatively charged donor center D^- . The binding energy of the second electron in the D^- center is usually quite small on the order of ~ 0.055 of the donor binding energy. This energy will be higher, however, in the type I CdSe/CdS core/shell structure, due

to an additional attractive potential (created by the CdSe core) for an electron. Finally, a biexciton in these structures looks like the helium atom, with two holes localized in the core and two electrons with opposite spins occupying the same orbit.

In this paper, we have calculated the binding energy and the fine structure of the exciton in CdSe/CdS NCs with a very thick shell as a function of the CdSe/CdS conduction band offset and the core radius. The calculations takes into account the complex structure of the CdSe valence band and inter-particle Coulomb and exchange interaction. We have also developed a general theory describing the fine structures and radiative decay time of positively and negatively charged trions. Using this theory we have calculated optical spectra of trions in giant CdSe/CdS core/shell NCs as a function of conduction-band offset and core radius.

This paper is organized as follows: In Section II and III we describe the energy spectra and wave functions of one and two holes localized in the CdSe core. In Section IV we discuss the energy and the wave function of an electron in a central symmetrical potential created by localized holes and the conduction band offset. In Section V we derive the wave functions and the energy of excitons and positively charged trions. In Section VI we discuss the fine structure of these excitons and trions. In Section VII we calculate the binding energy of the negatively-charged trions. In Section VIII we consider the radiative decay of all exciton complexes. Finally, we discuss obtained results and compare them with available experimental data in Section IX.

II. HOLE ENERGY SPECTRA AND WAVE FUNCTIONS

In CdSe/CdS core shell nanocrystals, the valence band offset is substantially large and the holes are strongly confined in the CdSe core. For the heavy ground state holes this potential can be considered as infinitely high in the first approximation. The first quantum-size level of holes in a spherical NC of a semiconductor with the degenerate Γ_8 valence subband is a $1S_{3/2}$ state.¹⁷ This state has total angular momentum $\mathbf{j} = 3/2$ and it is fourfold degenerate with respect to its projection $M = 3/2, 1/2, -1/2, -3/2$ on the z axis.¹⁷ The wave functions of these four states can be written as¹⁸

$$\Psi_M^h = 2 \sum_{l=0,2} (-1)^{M-3/2} R_l(r) \sum_{m+\mu=M} \begin{pmatrix} l & 3/2 & 3/2 \\ m & \mu & -M \end{pmatrix} Y_{l,m} u_\mu^v, \quad (1)$$

where $\begin{pmatrix} i & k & l \\ m & n & p \end{pmatrix}$ are Wigner 3j-symbols, $Y_{l,m}(\theta, \phi)$ are spherical harmonics defined in Ref.19, and u_μ^v ($\mu = \pm 1/2, \pm 3/2$) are the Bloch functions of the fourfold degenerate valence band Γ_8 ²⁰. The radial functions $R_0(r)$ and $R_2(r)$ corresponding to an impenetrable barrier at the CdSe/CdS interface with radius a can be written in explicit form following Refs. 21 and 22:

$$\begin{aligned} R_2(r) &= \frac{A}{a^{3/2}} \left[j_2(\varphi r/a) + \frac{j_0(\varphi)}{j_0(\varphi\sqrt{\beta})} j_2(\varphi\sqrt{\beta}r/a) \right], \\ R_0(r) &= \frac{A}{a^{3/2}} \left[j_0(\varphi r/a) - \frac{j_0(\varphi)}{j_0(\varphi\sqrt{\beta})} j_0(\varphi\sqrt{\beta}r/a) \right], \end{aligned} \quad (2)$$

where j_0 and j_2 are spherical Bessel functions, the constant A is determined by the normalization condition $\int_0^a dr r^2 [R_0^2(r) + R_2^2(r)] = 1$ and $\beta = m_l/m_h$ is the ratio of light to heavy hole effective masses: m_l and m_h , respectively. The dimensionless parameter φ is a first root of the equation $j_0(\varphi)j_2(\sqrt{\beta}\varphi) + j_2(\varphi)j_0(\sqrt{\beta}\varphi) = 0$, and describes the energy of the lowest hole level²²: $E_{1S_{3/2}} = \hbar^2\varphi^2/(2m_h a^2)$.

The assymetry effects, which include the intrinsic assymetry of the hexagonal lattice structure of the crystal's field,²¹ and the nonspherical shape of the NC²³, split the four-fold degenerate hole state into two two-fold degenerate states with $|j_z| = 3/2$ and $|j_z| = 1/2$, respectively:

$$E_{1S_{3/2}, j_z} = E_{1S_{3/2}} - \frac{\Delta(\beta, a)}{2} (j_z^2 - 5/4), \quad (3)$$

where $\Delta(\beta, a) = \Delta_{\text{int}}(\beta) + \Delta_{\text{sh}}(\beta, a)$ where Δ_{int} and Δ_{sh} are the intrinsic and size dependent shape contributions which can be found, for example, in Ref. 24.

III. TWO HOLE ENERGY SPECTRA AND WAVE FUNCTIONS

Before considering the positively charged excitons, which can be observed in NCs with an extra hole, let us consider the energy spectra of two holes localized in the CdSe core. The application of the Pauli exclusion principle to the two holes occupying the $1S_{3/2}$ level is nontrivial. Generally, the two holes with momentum $|\mathbf{j}_1| = |\mathbf{j}_2| = 3/2$ according to the momentum summation rule $\mathbf{J} = \mathbf{j}_1 + \mathbf{j}_2$ could form four states with the total angular momentum $J = 3, 2, 1$ and 0 . The wave functions of these states can generally be written as

$$\Phi_{J, J_z}^{2h}(\mathbf{r}_1, \mathbf{r}_2) = (-1)^{J_z} \sqrt{2J+1} \sum_{M_1+M_2=J_z} \begin{pmatrix} 3/2 & 3/2 & J \\ M_1 & M_2 & -J_z \end{pmatrix} \Psi_{M_1}^h(\mathbf{r}_1) \Psi_{M_2}^h(\mathbf{r}_2), \quad (4)$$

where J_z is the projection of the total momentum \mathbf{J} on the z axis. The Pauli hole permutation requirement applied to the wave function described by Eq. (4), however, allows only the two nontrivial solutions. As a result, the two holes occupying the $1S_{3/2}$ level can only be in a 5-fold degenerate state with total momentum $J = 2$ and a state with $J = 0$.^{24,25}

Hole-hole exchange interaction splits the ground biexciton into the two states with total momentum $J = 2$ and $J = 0$. The straightforward calculation of the $h-h$ Coulomb interaction with the functions from Eq. (4) gives the energy of the corresponding levels:

$$E_J(\beta) = E_{2h}(\beta) + \Delta_{\text{exch}}(\beta) \left(\frac{5}{4} - \frac{J(J+1)}{6} \right) \quad (5)$$

where $E_{2h}(\beta) = 2E_{1S_{3/2}} + E_{\text{Coul}}^{2h}$ is the band-edge energy of the two-hole state taking into account the direct Coulomb repulsion only, $\Delta_{\text{exch}}(\beta) = E_0(\beta) - E_2(\beta)$ is the exchange splitting and can be written in the following form^{24,25}

$$\Delta_{\text{exch}}(\beta) = \frac{e^2}{\kappa} \cdot \frac{32}{25} \int \int r_1^2 r_2^2 dr_1 dr_2 \frac{r_{\leq}^2}{r_{>}^3} R_0(r_1)R_2(r_1)R_0(r_2)R_2(r_2), \quad (6)$$

where κ is the dielectric constant of the semiconductor and $r_{<} = \min\{r_1, r_2\}$, $r_{>} = \max\{r_1, r_2\}$. The direct Coulomb interaction energy is given by

$$E_{\text{Coul}}^{2h}(\beta) = \frac{e^2}{\kappa} \cdot \int \int r_1^2 r_2^2 dr_1 dr_2 \frac{1}{r_{>}} (R_0^2(r_1) + R_2^2(r_1))(R_0^2(r_2) + R_2^2(r_2)) - \frac{5}{8}\Delta_{\text{exc}}. \quad (7)$$

In the spherical NCs, the ground two hole state has total momentum $J = 2$.²⁵ In the case of the CdSe/CdS structure with impenetrable interface, when the wave functions are described by Eq. (2), the exchange splitting and Coulomb energy can be written as

$$\Delta_{\text{exch}}(\beta) = \frac{e^2}{\kappa a} \gamma(\beta), \quad E_{\text{Coul}}^{2h}(\beta) = \frac{e^2}{\kappa a} \chi(\beta). \quad (8)$$

In CdSe NCs, where $\beta \approx 0.28$, $\gamma(0.28) \approx 0.033$ ²⁴ and $\chi(0.28) \approx 1.92$.

The NC asymmetry, which lifts the degeneracy of the $1S_{3/2}$ hole state in Eq.(3), causes further splitting of the two hole states. The corresponding perturbation can be written as²⁴

$$\hat{H}_{\text{as}}^{2h} = \hat{H}_{\text{as}}^{1h}(\mathbf{r}_1) + \hat{H}_{\text{as}}^{1h}(\mathbf{r}_2) = -\frac{\Delta(\beta, a)}{2}(\hat{j}_{1z}^2 - 5/4) - \frac{\Delta(\beta, a)}{2}(\hat{j}_{2z}^2 - 5/4), \quad (9)$$

where \hat{j}_{1z} and \hat{j}_{2z} are the operators of hole momentum projection acting on the first and second hole, respectively. The resulting two-hole states are described in Ref. 24. The ground two-hole state has angular momentum projection of $J_z = 0$ and energy

$$E_0^- = E_2(\beta, a) + \frac{\Delta_{\text{exch}}(\beta, a)}{2} - \sqrt{\left(\frac{\Delta_{\text{exch}}(\beta, a)}{2} \right)^2 + \Delta(\beta, a)^2}, \quad (10)$$

The first excited state has $J_z = \pm 1$, and ± 2 and energy E_2 , which is not affected by perturbations connected with NC asymmetry. Finally, the upper state has $J_z = 0$ and the energy

$$E_0^+ = E_0(\beta, a) - \frac{\Delta_{\text{exch}}(\beta, a)}{2} + \sqrt{\left(\frac{\Delta_{\text{exch}}(\beta, a)}{2}\right)^2 + \Delta(\beta, a)^2}, \quad (11)$$

Two-hole wave functions $\Phi_0^{2h,\pm}$ (for the energies E_0^\pm) and $\Phi_{\pm 1,\pm 2}^{2h}$ (for the fourfold degenerate intermediate level E_2) are given by²⁴

$$\begin{aligned} \Phi_0^{2h,\pm}(\mathbf{r}_{h1}, \mathbf{r}_{h2}) &= \frac{1}{2} [(B_2^\pm + B_0^\pm) (\Psi_{3/2}^h(\mathbf{r}_{h1})\Psi_{-3/2}^h(\mathbf{r}_{h2}) - \Psi_{-3/2}^h(\mathbf{r}_{h1})\Psi_{3/2}^h(\mathbf{r}_{h2})) + \\ &\quad (B_2^\pm - B_0^\pm) (\Psi_{1/2}^h(\mathbf{r}_{h1})\Psi_{-1/2}^h(\mathbf{r}_{h2}) - \Psi_{-1/2}^h(\mathbf{r}_{h1})\Psi_{1/2}^h(\mathbf{r}_{h2}))], \\ \Phi_{\pm 1}^{2h}(\mathbf{r}_{h1}, \mathbf{r}_{h2}) &= \pm \frac{1}{\sqrt{2}} (\Psi_{\pm 3/2}^h(\mathbf{r}_{h1})\Psi_{\mp 1/2}^h(\mathbf{r}_{h2}) - \Psi_{\mp 1/2}^h(\mathbf{r}_{h1})\Psi_{\pm 3/2}^h(\mathbf{r}_{h2})), \\ \Phi_{\pm 2}^{2h}(\mathbf{r}_{h1}, \mathbf{r}_{h2}) &= \pm \frac{1}{\sqrt{2}} (\Psi_{\pm 3/2}^h(\mathbf{r}_{h1})\Psi_{\pm 1/2}^h(\mathbf{r}_{h2}) - \Psi_{\pm 1/2}^h(\mathbf{r}_{h1})\Psi_{\pm 3/2}^h(\mathbf{r}_{h2})), \end{aligned} \quad (12)$$

where

$$B_0^\pm = \mp \frac{2\Delta}{\sqrt{4\Delta^2 + D_\pm^2}}, \quad B_2^\pm = \sqrt{1 - (B_0^\pm)^2}, \quad (13)$$

with $D_\pm = \Delta_{\text{exch}} \mp \sqrt{\Delta_{\text{exch}}^2 + 4\Delta^2}$.

IV. ELECTRON ENERGY SPECTRA AND WAVE FUNCTIONS

In Section II above we have considered holes in the CdSe/CdS core/shell NCs assuming that they are very strongly confined in the CdSe core. In that case their wave functions are not modified by the Coulomb interaction with the electron or by the hole-hole interaction, and are solely determined by the radius of the CdSe core. On the contrary, the conduction band offset in such structures is known to be small and even the sign of the band offset is not confirmed. As a result, the band offset itself does not localize (or only weakly localizes) an electron in the CdSe core. The attractive Coulomb potential created by the holes plays an important role in electron localization at the center of the core/shell NC structures.

We will show in the next section that the attractive Coulomb potential created by holes localized in a *spherically symmetrical* CdSe core does not have spherical symmetry. In the first approximation, however, the ground electron state is described by the wave function of S symmetry, which can be written as

$$\Psi_{\pm 1/2}^e(\mathbf{r}) = R_e^Z(r)Y_{00}(\Theta)u_{\pm 1/2}^c, \quad (14)$$

where $u_{S_z}^c = |S, S_z\rangle$ are the Bloch wave functions of the conduction band and $S_z = \pm 1/2$ is the electron spin projection. The radial wave function $R_e^Z(r)$ is described by the radial Hamiltonian

$$\begin{aligned} \hat{H}_r^Z(r) &= -\frac{\hbar^2}{2m_e(r)} \frac{1}{r^2} \frac{d}{dr} \left(r^2 \frac{d}{dr} \right) + V^Z(r), \\ m_e(r) &= m_{CdSe}, \quad V^Z(r) = V_{Coul}^Z(r) + U_{off}, \quad r < a, \\ m_e(r) &= m_{CdS}, \quad V^Z(r) = V_{Coul}^Z(r). \quad r > a \end{aligned} \quad (15)$$

Here U_{off} is the conduction band offset (CBO) ($U_{off} > 0$ in type II structures and $U_{off} < 0$ in type I structures), m_{CdSe} and m_{CdS} are the electron effective masses in CdSe and CdS, correspondingly, and $V_{Coul}^Z(r)$ is the effective Coulomb potential of one ($Z = 1$) or two ($Z = 2$) holes acting on an electron. We use $Z = 0$ to describe the "free" electron problem in the case of the neutral core.

The radial wave function $R_e^Z(r)$ is completely defined by Eq. (15) and the standard boundary conditions at the CdSe/CdS interface $r = a$:

$$\begin{aligned} R_e^Z(r)|_{r < a} &= R_e^Z(r)|_{r > a}, \\ \frac{1}{m_{CdSe}} \frac{dR_e^Z(r)}{dr} \Big|_{r < a} &= \frac{1}{m_{CdS}} \frac{dR_e^Z(r)}{dr} \Big|_{r > a}. \end{aligned} \quad (16)$$

Later we will need the radial function of the "free" resident electron, which remains in NCs after negative trion recombination. Its wave function $R_e^0(r)$ can be written as

$$R_e^0(r) = A \begin{cases} \frac{h_0^1(i\kappa a)}{j_0(ka)} j_0(kr) & r \leq a \\ h_0^1(i\kappa r) & r > a \end{cases} \quad (17)$$

where A is the normalization constant, h_0^1 is the spherical Hankel function,²⁶ $\kappa = \sqrt{-2m_{CdSe}E_e^0}/\hbar$, $k = \sqrt{2m_{CdS}(E_e^0 + U_{off})}/\hbar$ and E_e^0 is the electron ground state energy level calculated from the bottom of the CdS conduction band. This energy is described by the smallest solution of the following equation:

$$1 - ka \cot(ka) = \mu(1 + \kappa a) \quad (18)$$

where $\mu = m_{CdSe}/m_{CdS}$. It is important to note that even if CdSe/CdS core/thick shell NCs are Type I structures, the resident electron is not localized in the CdSe core with small radius a and is spread over the entire CdS shell. The electron localization occurs only if the power of a quantum well $w_0 = a\sqrt{2m_{CdSe}U_{off}}/\hbar$ is larger than w_0^{cr} , which is a solution of the following

equation: $\cot(w_0^{\text{cr}}) = (1 - \mu)/w_0^{\text{cr}}$. For $\mu = 1$ the electron delocalization occurs when $w_0^{\text{cr}} = \pi/2$, the condition which is identical to the standard expression for the critical depth of the 3D potential allowing the electron localization, $U_{\text{Off}} = \pi^2 \hbar^2 / (8m_{\text{CdSe}} a^2)$.²⁷ However, the large electron effective mass in CdS resulting in $\mu = 0.634$ allows the localization in the CdSe core with w_0 smaller than $\pi/2$: $\pi/2 > w_0 > w_0^{\text{cr}} = 1.296$.

V. DONOR-LIKE EXCITON AND POSITIVELY CHARGED TRION

The electron wave function is strongly modified by a long range Coulomb potential created by a hole or holes in the donor-like exciton or the positively charged trion in CdSe/CdS NCs with a small CBO. Electrons are bound to the CdSe core by a strong Coulomb potential of a single hole or two holes, $Z = 1, 2$ correspondingly, which are strongly confined by the core potential, similar to an electron in singly or doubly charged donors. This potential always leads to some binding of electrons to the CdSe core, even in type II CdSe/CdS core/shell structures. The attraction potential of holes is described by the distribution of the hole positive charge within the core of the radius a .

A. Hole charge distribution and Coulomb potential

The straightforward use of the hole wave function definition in Eq. (1) gives the charge distribution of the single hole state with $M = \pm 3/2$ and $M = \pm 1/2$ correspondingly:

$$\begin{aligned} \rho_{\pm 3/2}(\mathbf{r}) &= |\Psi_{\pm 3/2}^h(\mathbf{r})|^2 = \left(R_0(r)Y_{00} + \frac{1}{\sqrt{5}}R_2(r)Y_{20} \right)^2 + \frac{2}{5}R_2^2(r) (|Y_{2\pm 1}|^2 + |Y_{2\pm 2}|^2) , \\ \rho_{\pm 1/2}(\mathbf{r}) &= |\Psi_{\pm 1/2}^h(\mathbf{r})|^2 = \left(R_0(r)Y_{00} - \frac{1}{\sqrt{5}}R_2(r)Y_{20} \right)^2 + \frac{2}{5}R_2^2(r) (|Y_{2\mp 1}|^2 + |Y_{2\mp 2}|^2) , \end{aligned} \quad (19)$$

Using the definition of spherical harmonics, $Y_{l,m}$, from¹⁹ we arrive to

$$\rho_M(\mathbf{r}) = \frac{1}{4\pi} \left[R_0^2(r) + 2(|M| - 1)R_0(r)R_2(r)(1 - 3\cos^2\theta) + R_2^2(r) \right] . \quad (20)$$

The charge distribution of two *isotropic* holes with $\Delta = 0$, localized in CdSe core, $\rho_{J,J_z}^{2h}(\mathbf{r})$ can be obtained from the two-hole wave functions Φ_{J,J_z}^{2h} defined in Eq. (4):

$$\rho_{J,J_z}^{2h}(\mathbf{r}) = \int d^3r_{h1} d^3r_{h2} |\Phi_{J,J_z}^{2h}(\mathbf{r}_{h1}, \mathbf{r}_{h2})|^2 [\delta(\mathbf{r} - \mathbf{r}_{h1}) + \delta(\mathbf{r} - \mathbf{r}_{h2})] \quad (21)$$

To obtain the hole charge distribution for $\Delta \neq 0$ one has to use the two hole wave functions described in Eq. (12). The calculations show that for the four-time degenerate hole state E_2 , which is characterized by the angular momentum projections $J_z = \pm 1, \pm 2$, the charge distribution is spherical and is described as

$$\rho_{\pm 1, \pm 2}^{2h}(r) = \frac{2}{4\pi} [R_0^2(r) + R_2^2(r)] \quad (22)$$

For the upper, " E_0^+ ", and lower, " E_0^- ", two hole states with $J_z = 0$ similar calculations result

$$\rho_0^{2h, \pm}(\mathbf{r}) = \frac{2}{4\pi} [R_0^2(r) + R_2^2(r) + 2B_0^\pm B_2^\pm R_0(r)R_2(r)(1 - 3\cos^2\theta)] \quad (23)$$

In the limit $\Delta \gg \Delta_{exch}$ Eq. (23) is simplified significantly:

$$\rho_0^{2h, \pm}(r) = \frac{2}{4\pi} [R_0^2(r) + R_2^2(r) \mp R_0(r)R_2(r)(1 - 3\cos^2\theta)] . \quad (24)$$

Comparison of Eq. (24) with Eq. (20) shows clearly that in the case $\Delta \gg \Delta_{exch}$, the lowest level is created from two heavy holes, while the uppermost level is created by two light holes. Similar comparison of Eq. (22) with Eq. (20) shows that the middle level is always created by one light and one heavy hole.

One can show that only the spherical part of the hole charge distribution contributes to the ground S electron state in first order perturbation theory. For the single ($Z = 1$) and double ($Z = 2$) hole states this distribution can be written as

$$\rho_0^Z(r) = \frac{Z}{4\pi} [R_0^2(r) + R_2^2(r)] \quad (25)$$

The Coulomb potential created by the hole spherical charge distribution can be written as

$$V_{\text{Coul}}^Z(r) = -\frac{Ze^2}{\kappa} \int_0^a dr'^3 \frac{\rho_0^Z(r')}{|\mathbf{r} - \mathbf{r}'|} \quad (26)$$

where κ is the dielectric constant, which is considered to be the same in both CdSe and CdS. Equation (26) can be rewritten as:

$$V_{\text{Coul}}^Z(r) = -\frac{Ze^2 4\pi}{\kappa} \left[\frac{1}{r} \int_0^r dr' r'^2 \rho_0^Z(r') + \int_r^a dr' r' \rho_0^Z(r') \right] . \quad (27)$$

This potential outside the CdSe core, $r > a$, always has a standard Coulomb form, $V(r) = Ze^2/(\kappa r)$, due to the wave function normalization condition, $\int_0^a dr r^2 [R_0^2(r) + R_2^2(r)] = 1$. Inside the core $V'(r)|_{r=0} = 0$, and the potential depth $V(0) = -(Ze^2 4\pi/\kappa) \int_r^a dr r \rho_0^Z(r)$ depends only on the ratio β of the light- to heavy-hole effective masses. In CdSe where $\beta = 0.28$; $V(0) = 2.684Ze^2/(\kappa a)$.

B. Electron wave function and binding energy

We will consider only CdSe/CdS core/shell NCs with a very thick shell because these NCs show the most interesting and useful properties. From now on all calculations will be conducted for heterostructure with unlimited CdS shell thickness; later we will discuss the limitations of our approach.

The ground state of a weakly bound electron in the donor-like exciton or positively charged trion created in CdSe/CdS is described by the Hamiltonian of Eq. (15) with Coulomb potential, V_{Coul}^Z , described by Eq. (27). Introducing dimensionless distance from the NC center, $x = r/a$, and dimensionless energies $\bar{E} = E/(\hbar^2/2m_{\text{CdSe}}a^2)$, we obtain the dimensionless Hamiltonian,

$$\hat{H}_r^Z(x) = \begin{cases} -\frac{1}{x^2} \frac{d}{dx} \left(x^2 \frac{d}{dx} \right) + \frac{Z}{\eta_0} \bar{V}(x) + \bar{U}_{\text{off}} & , x < 1 \\ -\mu \frac{1}{x^2} \frac{d}{dx} \left(x^2 \frac{d}{dx} \right) + \frac{Z}{\eta_0} \bar{V}(x) & , x > 1 \end{cases} \quad (28)$$

for the radial component of the electron wave function, $R_e^Z(x)$. In Hamiltonian $\hat{H}_r(x)$ we use $\bar{V}(x) = 2V_{\text{Coul}}(r)/(Ze^2/\kappa a)$, $\bar{U}_{\text{off}} = U_{\text{off}}/(\hbar^2/2m_{\text{CdSe}}a^2)$. All energies are calculated from the bottom of the CdS conduction band, and the confinement potential U_{off} created by the conduction band offset is negative in type I, and positive in type II, CdSe/CdS hetero-structures. We also introduce the unitless parameter $\eta_0 = a_B/a$ that characterizes the strength of Coulomb potential created by holes, where $a_B = \hbar^2\kappa/(m_{\text{CdSe}}e^2)$ is the Bohr radius.

A central parabolic part of the hole potential described by Eq. (27) becomes important if Z/η_0 is large. The wave function of the 1S ground state should be close to the wave function of the harmonic oscillator. In the opposite case of small Z/η_0 , the core potential is weak and the electron moves mainly in the Coulomb-like potential at large distances from the core. To describe both above-mentioned limits, we select a trial radial function in the following form:

$$R_e^Z(\alpha, \zeta; x) = \begin{cases} (Ax^2 + B)e^{(1-x^2)/\alpha^2} & x \leq 1 \\ De^{(1-x)/\zeta} & x > 1 \end{cases} \quad (29)$$

where α and ζ are dimensionless variation parameters, which will be found using the variational principle, and constants A , B , and D , which are completely determined by the

interface boundary and normalization conditions. The standard boundary conditions at the CdSe/CdS interface ($x = 1$) described by Eq. (16) gives

$$R_e^Z(\alpha, \zeta; x) = \begin{cases} B e^{(1-x^2)/\alpha^2} \left[1 + x^2 \frac{(2\zeta - \alpha^2\mu)}{2(\alpha^2 - 1)\zeta + \alpha^2\mu} \right] & x \leq 1 \\ B e^{(1-x)/\zeta} \frac{2\alpha^2\zeta}{2(\alpha^2 - 1)\zeta + \alpha^2\mu} & x > 1, \end{cases} \quad (30)$$

where B can be found from the normalization condition $\int_0^\infty dx x^2 R_e^Z(\alpha, \zeta; x) = 1$ (see Appendix).

Using Eq. (28) we can find the expectation value for the energy, \bar{E}^Z , of one electron:

$$\langle \bar{E}^Z \rangle_e = \int_0^\infty R_e^Z(x) \hat{H}_r^Z(x) R_e^Z(x) x^2 dx \quad (31)$$

To simplify the calculation we approximate the potential, $\bar{V}(x)$ which is inside the core ($x < 1$) by the polynomial $\bar{V}(x) \approx p_0 + p_2x^2 + p_3x^3 + p_4x^4 + p_5x^5$, where $p_0 = -5.368$ and $p_1 = 0$ were selected to satisfy the exact potential properties at $x = 0$. Outside the core ($x > 1$) the potential is given by $\bar{V} = -2/x$ according to Eq.(27). The potential and the potential derivatives should be continuous at $x = 1$, which allows us to determine $p_4 = 14.84257478 - 3p_2 - 2p_3$ and $p_5 = -11.4740598 + 2p_2 + p_3$. Next, we vary the coefficients p_2 and p_3 to fit the polynomial to the function $\bar{V}(x)$, the form of which depends only on the parameter β . The best fit of $\bar{V}(x)$ for $\beta = 0.28$ was achieved using $p_2 = 10.6559838$ and $p_3 = -7.111613$. Figure 1 shows the dimensionless potential $\bar{V}(x)$. The COB is introduced via \bar{U}_{Off} . One can see that when the band offset is positive, the electron is pushed away from the CdSe core. The negative band offset added to the Coulomb attractive potential stimulates electron localization. The second hole localized in the CdSe core just increases the magnitude of the attractive potential by a factor of two.

Using this approximation we were able to develop an analytical expression for the electron binding energy $\langle \bar{E}^Z \rangle_e(\alpha, \zeta)$, via parameters α and ζ and find the absolute minimum of the total energy and a corresponding pair of ζ and α for given μ , η_0 , Z , and the band offset U_{Off} (see online Supplemental Material).

Figure 2 shows the binding energy of an electron for various core radii and band offsets, calculated for the cases when the CdSe core is charged with one ($Z = 1$) and two ($Z = 2$) holes. The energy is calculated from the bottom of the of the CdS conduction band. The size dependences are calculated for a CdSe core with a 2.5 nm radius and shown for five band

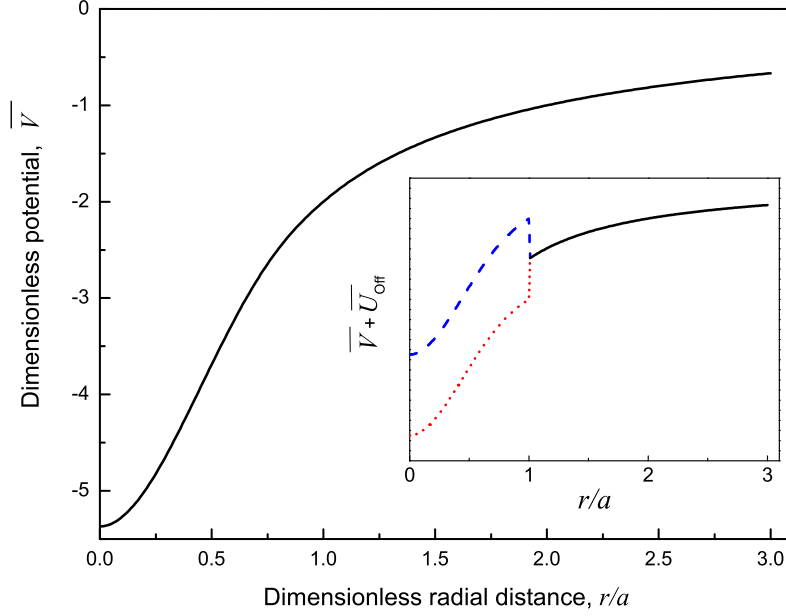


FIG. 1. Dimensionless Coulomb potential $\bar{V}(x)$ created by one hole ($Z = 1$). Insert shows schematically the total potential created by the sum of the Coulomb potential acting on the electron and the conduction band offset.

offsets: $u = 50, 0, -50, -100, -200$ meV. One can see that in NCs with small negative or positive band-offset, this energy decreases with a radius increase, while in the case of -100 and -200 meV, it increases following the bottom of the conduction band. The decrease of the binding energy with radius increase in NCs with small negative or positive band-offset is connected with the fact that electron motion in such NCs is controlled by Coulomb potential, which decreases with NC size.

Figure 2 shows the dependence of the electron binding energy on the band offset, \bar{U}_{Off} , in NCs with core radius 1.5, 2.5, and 3.5 nm radius for the single and doubly charged CdSe core. The band offset depends on temperature¹⁴, and the shift of the exciton line can be observed in temperature dependence.

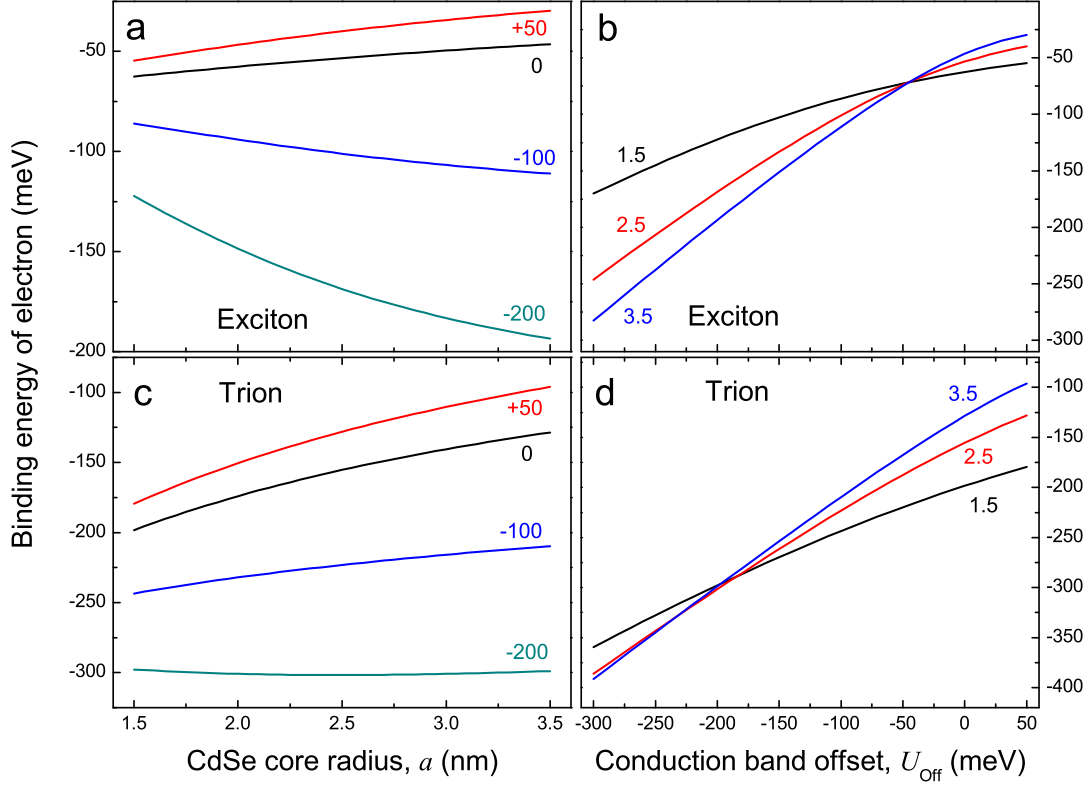


FIG. 2. Binding energy of an electron in the Coulomb potential created by one and two holes localized in the CdSe core calculated for various core radii and conduction band offsets. The dependence of the electron binding energy on the CdSe core radius, a , for one hole (Panel a) and two holes (Panel c). The dependence of the electron binding energy on the conduction band offset \bar{U}_{Off} for one (Panel b) and two holes (Panel d).

VI. THE FINE STRUCTURE OF EXCITONS AND POSITIVELY CHARGED TRIONS

The fine structure of the excitons and trions is strongly affected by the electron-hole exchange interaction, which can be written in spherical approximation as

$$H_{\text{exch}} = -\frac{2}{3}a_0^3\delta(\mathbf{r}_e - \mathbf{r}_h)\varepsilon_{\text{exch}}(\boldsymbol{\sigma} \cdot \mathbf{j}), \quad (32)$$

where, a_0 is the lattice constant, $\varepsilon_{\text{exch}}$ is the strength of the exchange interaction (in energy units), $\boldsymbol{\sigma}$ are the Pauli matrices, and $\mathbf{j} = j_x, j_y, j_z$ are three matrices of the momentum

3/2. The strength of the exchange interaction in cubic and hexagonal semiconductors can be determined from the bulk exciton fine structure. In CdSe this constant extracted from the bulk exciton splitting $\varepsilon_{\text{exch}} = 450 \text{ meV}$.²²

Averaging Eq. (32) over electron and hole wave functions in the basis of the 8-fold degenerate exciton state²², one can arrive at the following expression for the spin-spin exchange Hamiltonian between an electron and a hole:

$$H_{\text{exch}}^1 = -\eta_1 (\boldsymbol{\sigma} \cdot \boldsymbol{j}), \quad (33)$$

where the exchange parameter η_Z depends strongly on the number of holes in CdSe core:

$$\eta_Z = \frac{a_0^3}{6\pi} \varepsilon_{\text{exch}} \int_0^a dr r^2 [R_e^Z(r)]^2 [R_0^2(r) + 0.2R_2^2(r)], \quad (34)$$

due to the strong effect of the core charge on the electron radial function, $R_e^Z(r)$. The radial functions $R_e^Z(r)$ and $R_{0,2}(r)$ are defined in Eqs.(30) and (2), respectively. Integration in Eq. (34) goes only to the core radius a because in our approximation the hole wave function $R_{0,2}(r)$ vanishes at the CdSe/CdS interface. One can see from Eq. (34), that if an electron is only weakly localized in the CdSe core, then the parameter η is small. This parameter is proportional to $(a_0/a\zeta)^3 \ll 1$ where $a\zeta$ is a localization radius of the electron.

In Fig. (3)a we show the dependence of the exchange energy η_1 of the exciton as a function of the conduction band offset for several CdSe core radii. One can see that increase of U_{Off} leads to an increase of electron localization in the core always increases η_1 . Figure (3)b we show the dependence of exciton exchange energy η_1 as a function of the CdSe core radius for several NCs band offsets. For all reasonable set of radii, η_1 increases with the decrease of the NC radius.

The ground exciton state in spherical NC of zinc-blende semiconductors is characterized by the total exciton momentum $\mathbf{F} = \mathbf{j} + \mathbf{S}$. For the ground 5-fold degenerate Dark exciton state $F = 2$, and for the excited 3-fold degenerate Bright exciton state $F = 1$. In cubic semiconductor NCs with nonspherical shape and NCs with wurzite lattice structure these states are split into 5 excitons, each of them characterized by the projection of the total momentum on the hexagonal axis F_z .²² The respective wave functions are constructed from the hole functions of Eq. (1) and electron functions of Eq. (14), with the radial functions $R_e^{Z=1}$ for the electron moving in the Coulomb potential $V_{\text{Coul}}^{Z=1}$ created by one hole localized in the CdSe core.

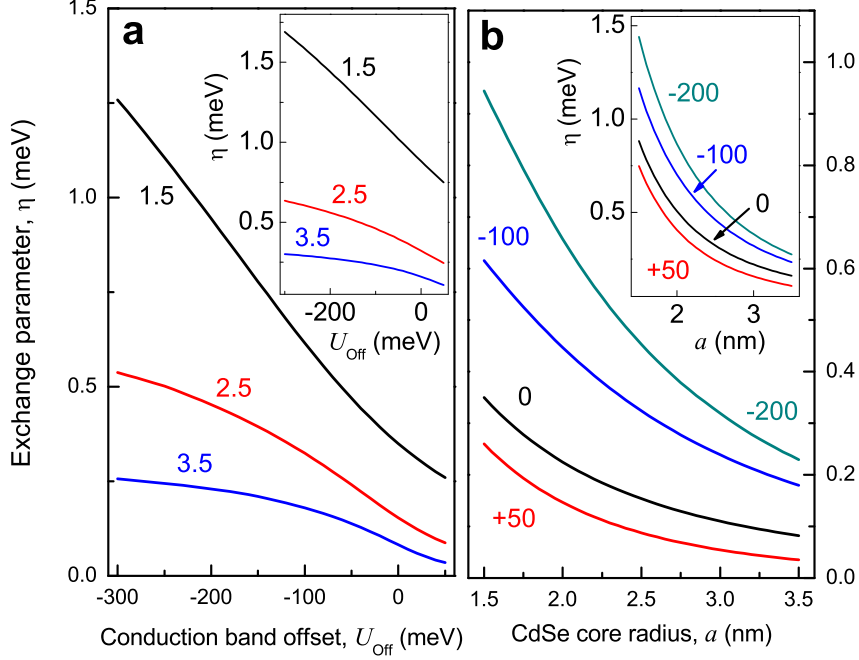


FIG. 3. Dependence of the exciton exchange parameter η_1 on the conduction band offset, U_{off} (a), and CdSe core radius, a (b). Insets show the same dependences for the trion exchange parameter η_2 .

The band edge exciton fine structure is completely characterized by two parameters η_1 and $\Delta(a, \beta)$ defined above. In spherical cubic NCs, the splitting between Bright and Dark excitons is given by $E_2 - E_1 = 4\eta_1$. In the case corresponding to $\Delta(a, \beta) \gg \eta_1$, the splitting between the ground Dark exciton with $F_z = \pm 2$ and the first excited Bright exciton with $F_z = \pm 1$ is $3\eta_1$. The last case is most probably realized in presently grown CdSe/CdS NCs.¹⁵ In the more general case, corresponding to $\Delta(a, \beta) \sim \eta_1$, the exciton fine structure is described by expressions which can be found in Refs. 22, 24, and 28.

The operator for the electron-hole exchange interaction in the positively charged trion can be written as

$$H_{\text{exch}}(\mathbf{r}_1) + H_{\text{exch}}(\mathbf{r}_2) = -\frac{2}{3}a_0^3\epsilon_{\text{exch}} [\delta(\mathbf{r}_e - \mathbf{r}_1)(\boldsymbol{\sigma} \cdot \mathbf{j}_1) + \delta(\mathbf{r}_e - \mathbf{r}_2)(\boldsymbol{\sigma} \cdot \mathbf{j}_2)] \quad (35)$$

where \mathbf{r}_1 , \mathbf{r}_2 and \mathbf{j}_1 , \mathbf{j}_2 are coordinates and spin matrices of two holes, respectively. The averaging of Eq. (35) over radial components of the two hole and electron wave functions

results in the effective electron-hole spin exchange Hamiltonian

$$H_{\text{exch}} = -2\eta_2(\boldsymbol{\sigma} \cdot \mathbf{J}), \mathbf{J} = \mathbf{j}_1 + \mathbf{j}_2, \quad (36)$$

where η_2 is defined in Eq. (34). The dependences of the trion exchange parameter η_2 on the core radius and the conduction band offset are shown in insets of Fig. (3). One can see that due to stronger attraction of the electron to the CdSe cores caused by the second hole, the trion's η_2 are larger than those for the exciton.

In the absence of the hole level splitting ($\Delta(\beta, a) = 0$), the states of the positively charged trion are characterized by the total momentum $\mathbf{G} = \mathbf{j}_1 + \mathbf{j}_2 + 1/2\boldsymbol{\sigma} = \mathbf{J} + \mathbf{S}$ and the trion wave functions can be generally found as

$$\Phi_{G,g}^{tr}(\mathbf{r}_e, \mathbf{r}_{h1}, \mathbf{r}_{h2}) = (-1)^{g-1/2} \sqrt{2G+1} \sum_{J_z+S_z=g} \begin{pmatrix} J & 1/2 & J \\ J_z & S_z & -g \end{pmatrix} \Phi_{J,J_z}^{2h}(\mathbf{r}_{h1}, \mathbf{r}_{h2}) \Psi_{S_z}^e(\mathbf{r}_e), \quad (37)$$

where g is the projection of the total momentum \mathbf{G} on the z axis, $S_z = \pm 1/2$ is the projection of the electron spin on the z axis, Φ_{J,J_z}^{2h} is the two-hole wave function described by Eq. (4), and $\Psi_{S_z}^e$ is the electron wave function described by Eq. (14) with the radial function R_e^2 for the electron moving in the Coulomb potential created by two holes. The ground trion state has total momentum $G = 5/2$ and the energy $E_{5/2} = E_2 - 2\eta_2$; the next one has $G = 3/2$ with the energy $E_{3/2} = E_2 + 3\eta_2$; and, finally, the upper state has $G = 1/2$ with the energy $E_{1/2} = E_0$. The last trion state is not affected by electron hole exchange interaction because the electron interaction with two different holes exactly compensate each other. The splitting of the two lowest hole states E_2 caused by the exchange interaction is $E_{5/2} - E_{3/2} = 5\eta_2$. The order of two excited trion states depends on the relative strength of electron-hole or hole-hole exchange interactions. All these trion states are twofold degenerate with respect of the momentum projection g , and their wave functions, $\Phi_{G,g}^{tr}$, can be written

$$\begin{aligned} \Phi_{1/2,\pm 1/2}^{tr} &= \Phi_{0,0}^{2h} \Psi_{\pm 1/2}^e, \quad \Phi_{3/2,\pm 1/2}^{tr} = \pm \sqrt{\frac{3}{5}} \Phi_{2,\pm 1}^{2h} \Psi_{\mp 1/2}^e \mp \sqrt{\frac{2}{5}} \Phi_{2,0}^{2h} \Psi_{\pm 1/2}^e, \\ \Phi_{3/2,\pm 3/2}^{tr} &= \pm \sqrt{\frac{1}{5}} (2\Phi_{2,\pm 2}^{2h} \Psi_{\mp 1/2}^e - \Phi_{2,\pm 1}^{2h} \Psi_{\pm 1/2}^e), \quad \Phi_{5/2,\pm 1/2}^{tr} = \sqrt{\frac{2}{5}} \Phi_{2,\pm 1}^{2h} \Psi_{\mp 1/2}^e + \sqrt{\frac{3}{5}} \Phi_{2,0}^{2h} \Psi_{\pm 1/2}^e, \\ \Phi_{5/2,\pm 3/2}^{tr} &= \sqrt{\frac{1}{5}} (\Phi_{2,\pm 2}^{2h} \Psi_{\mp 1/2}^e + 2\Phi_{2,\pm 1}^{2h} \Psi_{\pm 1/2}^e), \quad \Phi_{5/2,\pm 5/2}^{tr} = \Phi_{2,\pm 2}^{2h} \Psi_{\pm 1/2}^e, \end{aligned} \quad (38)$$

When the ground state of holes is split by a crystal field or when the NC shape is asymmetric, the related perturbation can be written in the basis of the trion functions of Eq. (38). The perturbation does not mix the the trion state with different signs of the spin projections. For the positive spin projections ($g = 5/2, 3/2$, and $1/2$) the perturbation has the following form:

$$\left(\begin{array}{c|cccccc} & |1/2, 1/2\rangle & |3/2, 1/2\rangle & |5/2, 1/2\rangle & |3/2, 3/2\rangle & |5/2, 3/2\rangle & |5/2, 5/2\rangle \\ \hline |1/2, 1/2\rangle & E_0 & \sqrt{\frac{2}{5}}\Delta & -\sqrt{\frac{3}{5}}\Delta & 0 & 0 & 0 \\ |3/2, 1/2\rangle & \sqrt{\frac{2}{5}}\Delta & E_2 + 3\eta_2 & 0 & 0 & 0 & 0 \\ |5/2, 1/2\rangle & -\sqrt{\frac{3}{5}}\Delta & 0 & E_2 - 2\eta_2 & 0 & 0 & 0 \\ |3/2, 3/2\rangle & 0 & 0 & 0 & E_2 + 3\eta_2 & 0 & 0 \\ |5/2, 3/2\rangle & 0 & 0 & 0 & 0 & E_2 - 2\eta_2 & 0 \\ |5/2, 5/2\rangle & 0 & 0 & 0 & 0 & 0 & E_2 - 2\eta_2 \end{array} \right) \quad (39)$$

A very similar matrix describes the perturbation created by nonzero Δ on the states with negative angular momentum projections: $g = -5/2, -3/2$, and $-1/2$. That matrix can be obtained by replacing states $|G, g'\rangle$ in Eq.(39) by states with $|G, -g'\rangle$, where $g' = 5/2, 3/2$, and $1/2$. The only difference is the sign of the matrix element taken between states $|1/2, -1/2\rangle$ and $|3/2, -1/2\rangle$, which in the last case is $-\sqrt{2/5}\Delta$.

One can see from Eq. (39), that NC asymmetry does not affect the three trion states $|5/2, \pm 5/2\rangle$, $|5/2, \pm 3/2\rangle$ and $|3/2, \pm 3/2\rangle$. The energies of these states are

$$E_{5/2} = E_2 - 2\eta_2, \quad E_{3/2} = E_2 + 3\eta_2, \quad (40)$$

and their wave functions, $\Phi_{3/2, \pm 3/2}^{tr}$ for $E_{3/2}$, and $\Phi_{5/2, \pm 3/2}^{tr}$ and $\Phi_{5/2, \pm 5/2}^{tr}$ for $E_{5/2}$ are the same as in the spherical case.

The other three trion states, $E_{1/2}^{\pm}$ and $E_{1/2}$ can be found as solutions of the following third order equation:

$$(E_2 - E - 2\eta_2)(E_2 - E + 3\eta_2)(E_0 - E) - \Delta^2(E_2 - E + \eta_2) = 0, \quad (41)$$

In the case of small electron-hole and hole-hole exchange interactions $\eta_2 \ll \Delta$, $\Delta_{exc} \ll \Delta$, the approximate solutions of Eq. (41) yield

$$E_{1/2}^{\pm} \approx E_0^{\pm} \approx E_2 + \Delta_{exc}/2 \pm \Delta, \quad E_{1/2} \approx E_2 + \eta_2. \quad (42)$$

The wave functions of these trion states are $\Phi_{\pm 1/2}^{tr,\pm} = \Phi_0^{2h,\pm} \Psi_{\pm 1/2}^e$ and $\Phi_{\pm 1/2}^{tr} = \Phi_{2\pm 1}^{2h} \Psi_{\mp 1/2}^e$, respectively.

In the limit of small exchange interaction, the order of the trion levels is independent of the relation between Δ_{exc} and η_2 . The fine structure of the positively charged trion is, ordered upward in energy, the ground twofold degenerate $E_{1/2}^-$ level, followed by the fourfold degenerate $E_{5/2}$ level, followed by the twofold degenerate $E_{1/2}$ and $E_{3/2}$ levels, and finally by the upper twofold degenerate $E_{1/2}^+$ level. The lowest and the uppermost trion states in the limit of large Δ are formed from the lowest and uppermost two-hole states with a total zero momentum projection of two holes $J_z = 0$, while all intermediate states are formed from the medium fourfold degenerate two-hole level with $J_z = \pm 1, \pm 2$. The medium level of the trion would be eightfold degenerate if one neglected the splitting caused by the electron-hole exchange interaction proportional to η_2 .

The limit of small exchange interaction should describe quite well the CdSe/CdS NCs which have a core radius ~ 20 Å. In these NCs, the hole-hole exchange interaction, $\Delta_{exc} \sim 5$ meV and $\Delta(\beta, a) \sim 20$ meV. The calculations of the electron-hole exchange interaction in Fig. 3 show that η_2 is also much smaller than $\Delta(\beta, a)$.

VII. NEGATIVELY CHARGED TRIONS

Let us consider now a negatively charged trion formed by the optically excited electron-hole pair and resident electron. The total energy of the negatively charged trion can be generally described as a sum of the two total energies of electrons interacting with the hole described in our case by Eq. (31) and the energy of the electron repulsion. In the case of the small conduction band offsets, the binding energy of the trion is mainly controlled by electron-electron and electron-hole Coulomb interactions as is true for the negatively charge hydrogen atom. The resulting binding energy in such a case is significantly smaller than the binding energy of the exciton because the Coulomb attraction between a second electron and the hole is almost exactly compensated by the Coulomb repulsion between electrons.

The studies of negatively charged hydrogen atoms (see for example Ref. 29) demonstrate that the binding state of doubly charged atom exist only for a singlet state of two electrons occupying the two radial orbits of S symmetry. This requirement decreases the Coulomb repulsion energy between two electrons. That is why we select the two-electron

wave functions of the negative trion $\Psi_{2e}(\mathbf{r}_1, \mathbf{r}_2)$ as the product of the singlet spin wave function (antysymmetrical) and symmetrical radial function of two S -symmetry electrons in the following form:

$$\Psi_{2e}(\mathbf{r}_1, \mathbf{r}_2) = \frac{1}{\sqrt{2}}(u_{1/2}^c(e1)u_{-1/2}^c(e2) - u_{-1/2}^c(e1)u_{1/2}^c(e2))Y_{00}(\Theta_{e1})Y_{00}(\Theta_{e2})R_{2e}(r_1, r_2), \quad (43)$$

where R_{2e} is defined as

$$R_{2e}(r_1, r_2) = A_{2e}[R_e^1(\alpha_1, \zeta_1; r_1/a)R_e^1(\alpha_2, \zeta_2; r_2/a) + R_e^1(\alpha_1, \zeta_1; r_2/a)R_e^1(\alpha_2, \zeta_2; r_1/a)] \quad (44)$$

with $R_e^1(\alpha, \zeta; r/a)$ defined in Eq. (30) and A_{2e} defined by the normalization condition $\int_0^\infty \int_0^\infty |R_{2e}(r_1, r_2)|^2 r_1^2 dr_1 r_2^2 dr_2 = 1$.

Using this approach we can write down the total dimensionless energy of two electrons in the trion

$$\langle \bar{E} \rangle_{2e} = 2 \int_0^\infty R_{2e}(r_1, r_2) \hat{H}_r(r_1) R_{2e}(r_1, r_2) \frac{d^3 r_1}{4\pi} \frac{d^3 r_2}{4\pi} + E_{\text{Coul}}^{2e}, \quad (45)$$

where the repulsion energy between two electrons E_{Coul}^{2e} can be found as

$$E_{\text{Coul}}^{2e} = \frac{e^2}{\kappa} \int \frac{d^3 r_1}{4\pi} \frac{d^3 r_2}{4\pi} \frac{|R_{2e}(r_1, r_2)|^2}{|\mathbf{r}_1 - \mathbf{r}_2|} = \frac{e^2}{\kappa} \int r_1^2 dr_1 r_2^2 dr_2 \frac{R_{2e}^2(r_1, r_2)}{r_{>}} \quad (46)$$

The two-electron trial wave function defined in Eq.(44) is described by four fitting parameters, and it generally describes the electron motion on two radial orbits characterized by two different sets α_1, ζ_1 and α_2, ζ_2 . It is important to note that if $\alpha_1 \neq \alpha_2$ and $\zeta_1 \neq \zeta_2$, the energy of two electrons in Eq. (45) is not reduced to the kinetic energy and repulsion of uncorrelated electrons occupying two different orbits. The total energy of electrons has a contribution from the interference of both orbits and depends on all four parameters.

One can find the analytical expression of the expectation energy $\langle \bar{E} \rangle_{2e}$ as a function of four parameters in the online SM. This expression developed within *Mathematica* were used to find the binding energy of two electrons and a hole. The trion binding energy, which is the difference between the total energy of the trion and the binding energy of the exciton (see Fig. 2), is shown in Fig. 4 as a function of of the NC core radius and band offset.

One can see that for large negative values of U_{Off} , the CdSe/CdS NCs are well-defined type-I structures. The strong confinement allows the two electrons to occupy a ground state level with two opposite spins leading to a large trion binding energy (see Fig. 5). Decrease of $|U_{\text{Off}}|$ decreases the confinement, and the trion binding energy is mainly controlled by

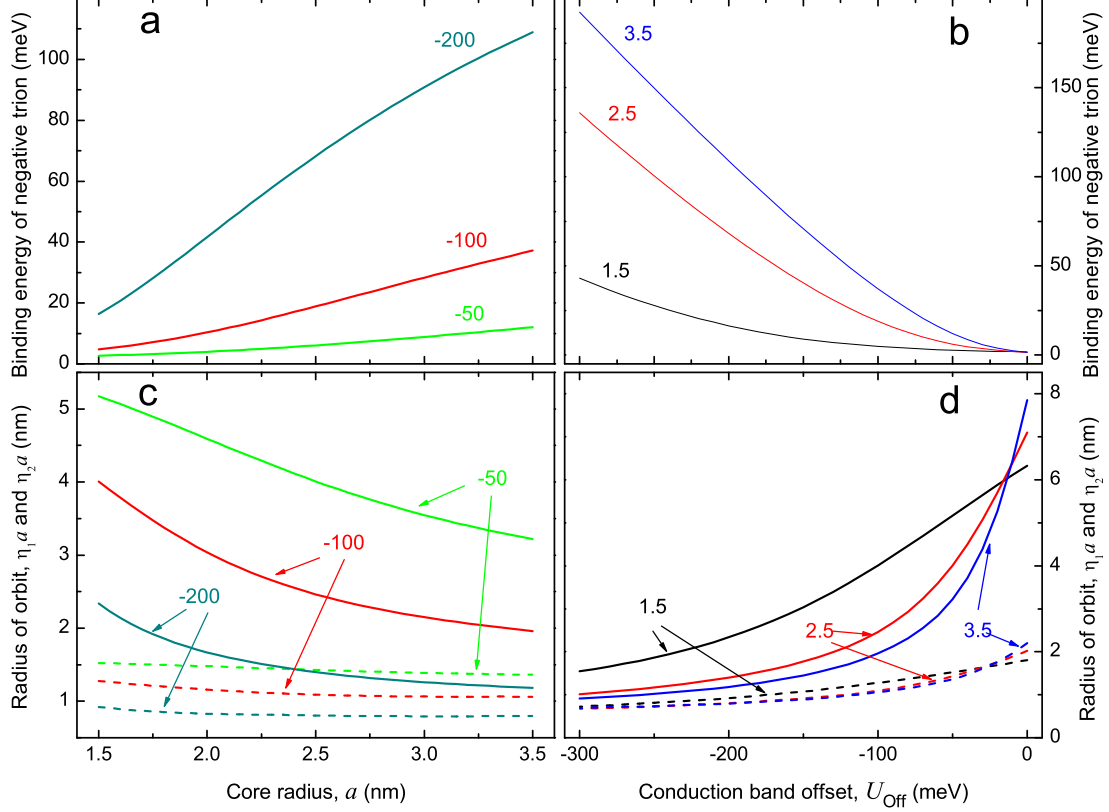


FIG. 4. Binding energy of the negatively charged trion in CdSe/CdS core thick/shell NCs. (a) - dependence of the binding on the core radius, a , calculated for three band offset $U_{\text{Off}} = -50, -100,$ and -200 meV. (b) - dependence of the binding on the band offset U_{Off} calculated for three radii $a = 1.5, 2.5,$ and 3.5 nm. Panels c and d show the dependence of the orbit radii $\zeta_1 a$ and $\zeta_2 a$ as functions of the core radius, a , and of the band offset U_{Off} , respectively.

the electron-electron and the electron-hole Coulomb interactions. The Coulomb repulsion between two electrons forces them to occupy different orbits, which reduces the repulsion and leads to a small, but positive binding energy for the trion. The orbits are characterized by the two radial wave functions, $R_e^1(\alpha_1, \zeta_1, r/a)$ and $R_e^1(\alpha_2, \zeta_2, r/a)$, the spatial extension of which is characterized by parameters $\zeta_1 a$ and $\zeta_2 a$. The radius of these two orbits is shown in Fig. 4c and 4d as a function of core radius and band offset. One can see that one of the orbits is mainly localized in the CdSe core while the other explores the CdS shell. The radius of the large orbit obviously increases with the decrease of $|U_{\text{Off}}|$ for any core

radius, as one can see in Fig. 4c. The CBO dependence shown in Fig. 4d is more complex, however. The radius of the external orbit is smaller in the NC with a large core radius at large CBOs, but it becomes larger at small CBOs. This unusual behavior is connected with the increased role that the hole Coulomb attraction potential plays in electron localization in core/shell NCs with a small CBO.

VIII. OPTICAL PROPERTIES OF EXCITONS AND TRIONS

A. Optical transition probabilities of the band edge excitons

The optical selection rule and the relative transition probabilities of the excitons in CdSe/CdS core shell NCs are described by Eqs. (25)–(28) of Ref. 22, where the square of the overlap integral, K , between the electron and hole wave functions should be written in more general form

$$K_{ex} = \left| \int dr r^2 R_e^1(r) R_0(r) \right|^2, \quad (47)$$

where R_e^1 is the electron radial function described in Eq. (29), with parameters α and ζ that maximized the exciton binding energy. In the CdSe/CdS core shell NCs, where the electron is not localized in the CdSe core, K_{ex} is a strong function of the band offset of the conduction band and of the core radius. In Figs. 5a and 5b we show the dependence of the exciton K_{ex} on the core radius and the band offset, respectively.

The experimentally observed increase of the the radiative decay time by a factor of two in the temperature interval from 0 to 150 K^{14,15,30} could be connected with a significant decrease of the conduction band offset between CdSe and CdS shell layers. The decrease of the absolute value of the negative band offset decreases K_{ex} , as one can see in Fig. 5 c, d and f. The radiative decay time of the optically active excitons is inversely proportional to K_{ex} and is directly proportional to the characteristic exciton decay time, as can be described by

$$\frac{1}{\tau_0} = \frac{8e^2\omega n_r P^2}{9m_0^2 c^2 \hbar} \mathcal{D} = \frac{\mathcal{D}}{\tau_0^i}, \quad (48)$$

where n_r is the refractive index of the media, c is the speed of light, $P = -i\langle S|\hat{p}_z|Z\rangle$ is the Kane transition matrix element, ω is the light frequency, and \mathcal{D} is the depolarization factor, which takes into account the decrease of the magnitude of the light electric field when it penetrates into the NC. In CdSe structures τ_0^i should be on the order of 1.7 ns.²⁸ This value

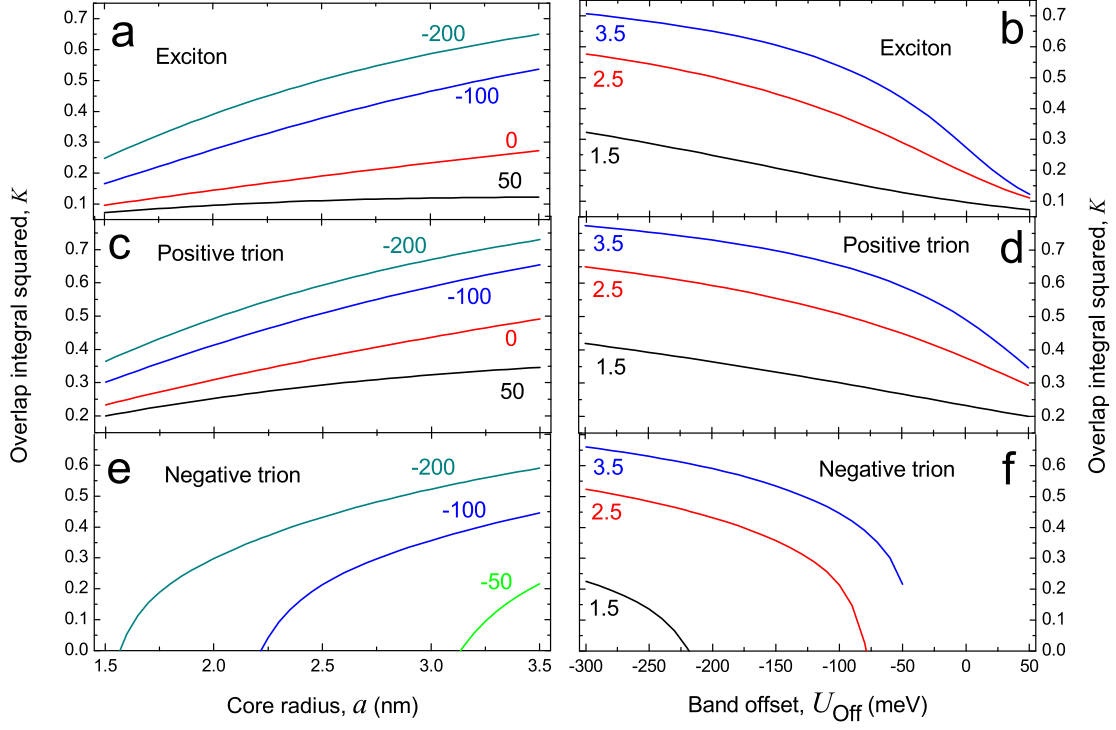


FIG. 5. Dependence of the square of the overlap integral, K , on the conduction band offset, U_{Off} (a), and (e); and CdSe core radius, a (b), (d), and (f), calculated for an exciton (a) and (b); a positively charged trion (c) and (d); and a negatively charged trion (e) and (f).

was estimated using $n_r = 1.5$, $\hbar\omega = 2$ meV and $2P^2/m_0 = 19.0$ eV. The depolarization factor \mathcal{D} generally depends on the NC shape and structure. In giant CdSe/CdS NCs the depolarization factor can be estimated using $\mathcal{D} = [3\epsilon/(2\epsilon + \epsilon_{\text{CdS}})]^2$ for spherical CdS NCs, where $\epsilon_{\text{CdS}} = 5.35$ is the high frequency dielectric constant of CdS and $\epsilon = n_r^2 = 2.25$ is the dielectric constant of the media surrounding the NC. This results in $\mathcal{D} \approx 0.47$.

The radiative decay times of the Bright band-edge excitons has a complicated dependence on the exciton exchange energy η_1 and the hole level splitting Δ .²² The expression for the decay time is significantly simplified when $\Delta \gg \eta_1$. In this limit the radiative decay time, τ_{ex} , of the first optically active exciton can be written as

$$\frac{1}{\tau_{ex}} = \frac{K_{ex}}{2\tau_0} \quad (49)$$

This case is realized in giant CdSe/CdS NCs, due to a small exchange energy. From Fig.5 one

can see that the overlap integral squared decreases by a factor of 2–3 when CBO decreases from 50 meV to 300 meV. This decrease of K_{ex} is consistent with observed changes in the radiative decay time. One can see also from Fig.5a that an increase of the core radius leads to a strong localization of an electron in the core and increases K_{ex} significantly. This in turn should shorten the radiative decay time.

B. Positively charged trion transition probabilities

The fine structure of the band-edge positive charge trions in NCs made of semiconductors with four-fold degenerate or quasi-degenerate valence bands (like CdSe, CdS, InAs, CdTe and etc.) generally consists of four doubly degenerate states $E_{1/2}^{\pm}$, $E_{3/2}$ and $E_{1/2}$ and one four-fold degenerated state $E_{5/2}$, whose energies we described above. All of these states are optically active and can decay radiatively with different decay times. This in principle could lead to a very complex dependence of the decay time on the temperature as a result of the thermal population of the different levels within the trion fine structure.

The resonant optical excitations of the positively charged trion in NCs with an extra hole and its radiative decay are determined by the probabilities of the optical transitions between one of a hole state, $1S_{3/2}$, with $M = \pm 1/2, \pm 3/2$ and the one of the trion states, $Tr [\pm 1/2^{\pm}; (3/2, \pm 3/2); (5/2, \pm 3/2); (5/2, \pm 5/2)$, and $(1/2, \pm 1/2)$. These probabilities are proportional to the following sum of the matrix element squared:

$$\begin{aligned}
 T(M, Tr) &= \sum_{i, j = 1, 2; i \neq j} |\langle \Psi_M^h(\mathbf{r}_{hi}) \delta(\mathbf{r}_e - \mathbf{r}_{hj}) | \mathbf{e} \hat{\mathbf{p}} | \Phi_{G,g}^{tr}(\mathbf{r}_e, \mathbf{r}_{h1}, \mathbf{r}_{h2}) \rangle|^2 \\
 &= 2 |\langle \Psi_M^h(\mathbf{r}_{h1}) \delta(\mathbf{r}_e - \mathbf{r}_{h2}) | \mathbf{e} \hat{\mathbf{p}} | \Phi_{G,g}^{tr}(\mathbf{r}_e, \mathbf{r}_{h1}, \mathbf{r}_{h2}) \rangle|^2 .
 \end{aligned} \tag{50}$$

The sum takes into account the probability of an electron recombination with two holes ($j = 1, 2$). The sum can be replaced by a factor of two because the matrix elements of the transitions with different hole states are identical, due the symmetrization of the two-hole wave function. Here \mathbf{e} is the polarization of the emitted or absorbed light, and the momentum operator $\hat{\mathbf{p}}$ acts only on the valence band Bloch functions. The calculation of $T(M, Tr)$ with the wave functions is straightforward but cumbersome, because the hexagonal axes of a NC ensemble are randomly oriented relative to the light propagation of emission directions. First, let us consider transition probabilities $T(M, Tr)$'s responsible for the radiative decay

of the ground and first excited trion state.

We will be considering here only the effect of linearly polarized light, which is sufficient for the description of the radiative decay. For linearly polarized light, $\mathbf{e}\hat{\mathbf{p}}$ in Eq. (50) can be written as

$$\mathbf{e}\hat{\mathbf{p}} = e_z\hat{p}_z + \frac{1}{2}[e_-\hat{p}_+ + e_+\hat{p}_-] \quad (51)$$

where z is the direction of the hexagonal axis of the NC, $e_{\pm} = e_x \pm ie_y$, $\hat{p}_{\pm} = \hat{p}_x \pm i\hat{p}_y$, and $e_{x,y}$ and $\hat{p}_{x,y}$ are the components of the polarization vector and the momentum operator, respectively, that are perpendicular to the NC hexagonal axis.

In studied CdSe/CdS core/shell NCs, the crystal field and shape asymmetry parameter Δ is much larger than the trion exchange parameter η . As a result the trion ground state is $1/2^-$. Let us calculate the transition probabilities $T(3/2, 1/2^-; \pi)$ and $T(-3/2, -1/2^-; \pi)$ between the trion ground state and the hole ground state $|M| = 3/2$ stimulated by the linear polarized light. Substituting Eq. (51) into Eq. (50) and using the trion and hole wave-functions, after some straightforward but cumbersome calculations gives the following:

$$T(-3/2, -1/2^-; \pi) = T(3/2, 1/2^-; \pi) = (B_2^- + B_0^-)^2 \frac{K_{tr^+} P^2}{4} \sin^2 \theta, \quad (52)$$

where θ is the angle between the vector polarization of light \mathbf{e} and the hexagonal axis of the NC, and where the trion overlap integral squared $K_{tr^+} = |\int dr r^2 R_e^{Z=2}(r) R_0(r)|^2$ is determined now by the electron wave function $R_e^{Z=2}$ of the trion, which is calculated for the Coulomb potential created by two holes. This radial function is described by Eq. (29), with parameters α and ζ that maximize the trion binding energy. The dependence of the overlap integral squared calculated for the positively charged trion is shown as functions of the CdSe core radius and CBO in Figs. 5 c and d.

Equation (52) describes the probability of the trion ground state radiative decay into the ground hole state. There is nothing, however, that prevents the trion decay into the light hole excited states with $M = \pm 1/2$. The photon emitted during such decay will be smaller (by an energy of about Δ) than the photon emitted during the ground-to-ground transition. This energy will be absorbed by the hole. The probability of observing such a red "shake up" line is determined by the four independent transition probabilities:

$$\begin{aligned} T(-1/2, -1/2^-; \pi) &= T(1/2, 1/2^-; \pi) = (B_2^- - B_0^-)^2 \frac{K_{tr^+} P^2}{3} \cos^2 \theta, \\ T(1/2, -1/2^-; \pi) &= T(-1/2, 1/2^-; \pi) = (B_2^- - B_0^-)^2 \frac{K_{tr^+} P^2}{12} \sin^2 \theta, \end{aligned} \quad (53)$$

which are much smaller than the probability of the observation of the main line, because $(B_2^- - B_0^-)^2 \ll (B_2^- + B_0^-)^2$ for large Δ .

Summing up the probabilities of the trion radiative decay into the ground and excited hole states over all light polarizations, we obtain the radiative recombination rate of the trion ground state as

$$\frac{1}{\tau_{1/2^-}^{tr+}} = \frac{K_{tr+}}{2\tau_0}, \quad (54)$$

One can show that the uppermost trion excited state $1/2^+$ has the same radiative decay rate as the ground one ($\tau_{1/2^+}^{tr+} = \tau_{1/2^-}^{tr+}$) and they are different from the decay time of the first optically active exciton state only by the overlap integrals (see Eq. (49)). Comparison of the overlap integral squared for excitons and positively charged trions in Fig. 5 shows that in NCs with small conduction band offsets they became much larger for the trions due to stronger attraction of electrons to the CdSe core. Henceforth in this paper we will use notations for the decay times, which are related to the notation of corresponding levels of the positively charged trion: $\tau_{1/2^\pm}^{tr+}$, $\tau_{3/2}^{tr+}$ and $\tau_{1/2}^{tr+}$ and $\tau_{5/2}^{tr+}$.

We find the probability of the transitions from the excited trion states $(5/2, \pm 5/2)$ and $(5/2, \pm 3/2)$ to the hole $M = \pm 3/2$ state to be

$$T(\pm 3/2, (5/2, \pm 5/2); \pi) = \frac{K_{tr+} P^2}{6} \sin^2 \theta, \quad T(\pm 3/2, (5/2, \pm 3/2); \pi) = \frac{2K_{tr+} P^2}{3} \cos^2 \theta. \quad (55)$$

The transition to the hole ground state has an energy of about Δ larger than the main transition from the ground state.

The total transition probability from the trion $\pm 5/2$ states to the hole ground $\pm 1/2$ state is described by the sum of the two probabilities:

$$T(1/2, (5/2, 3/2); \pi) = T(-1/2, (5/2, -3/2); \pi) = \frac{K_{tr+} P^2}{10} \sin^2 \theta. \quad (56)$$

In the same limit of large Δ , transitions from the trion excited state to the hole excited state have nearly the same energy as the main transition from the ground to ground states.

When we average all possible crystal orientation and sum up Eqs. (55) and (56), we can find the radiative recombination rate of the trion excited state $E_{5/2}$:

$$\frac{1}{\tau_{5/2}^{tr+}} = \frac{3K_{tr+}}{5\tau_0}, \quad (57)$$

Similar calculations give us the radiative rates for $E_{1/2}$ and $E_{3/2}$ excited trion states:

$$\frac{1}{\tau_{1/2}^{tr+}} = \frac{2K_{tr+}}{3\tau_0}, \quad \frac{1}{\tau_{3/2}^{tr+}} = \frac{11K_{tr+}}{15\tau_0}. \quad (58)$$

The situation is significantly simplified in studied here CdSe/CdS core/shell NCs. Due to small value of $\eta \ll \Delta$, the second trion level is eightfold degenerate with an average decay rate of

$$\frac{1}{\tau_2^{tr+}} = \frac{1}{4} \left(\frac{2}{\tau_{5/2}^{tr+}} + \frac{1}{\tau_{1/2}^{tr+}} + \frac{1}{\tau_{3/2}^{tr+}} \right) = \frac{K_{tr+}}{2\tau_0}, \quad (59)$$

which coincides with the decay rate of the uppermost and lowest trion states $1/\tau_{1/2}^{tr+}$ (see Eq. (54)). As a result, the positive trion radiative decay time in CdSe/CdS core/shell NCs does not depend on thermo-population of the fine level structure and is temperature independent.

C. Negatively charged trion transition probabilities

The radiative decay time of the negatively charged exciton leaves a resident electron in NCs. In CdSe/CdS core/shell NCs, the wave function of the resident electron, R_e^0 , is very different from the electron wave functions of the negatively charged trion, which is mainly controlled by the Coulomb interactions. The different size of the electron and hole wave functions significantly decreases the overlap integral, which controls the rate of trion radiative decay.

The radiative decay and the resonant optical excitation of the negatively charged trion are determined by the probabilities of the optical transitions between the resident "free" electron state, with spin projection $S_z = \pm 1/2$ and radial wave function R_e^0 , and one of the trion states characterized by the hole momentum projection $M = \pm 3/2, \pm 1/2$. These probabilities are proportional to

$$T(S_z, M) = 2 |\langle \Psi_{S_z}^e(\mathbf{r}_1) \delta(\mathbf{r}_1 - \mathbf{r}_{e2}) | e \hat{\mathbf{p}} | \Psi_M^h(\mathbf{r}_h) \Psi_{2e}(\mathbf{r}_{e1}, \mathbf{r}_{e2}) \rangle|^2, \quad (60)$$

where the factor 2 is due to the sum over electron coordinates. The ground negative trion state is formed by the hole with $M = \pm 3/2$. The probability from the ground state is

$$T(-1/2, -3/2; \pi) = T(1/2, 3/2; \pi) = \frac{K_{tr-} P^2}{2} \sin^2 \theta. \quad (61)$$

Here,

$$K_{tr-} = \left| \int \int r_1^2 dr_1 r_2^2 dr_2 R_e^0(r_1) R_{2e}(r_1, r_2) R_0(r_2) \right|^2, \quad (62)$$

where R_{2e} is the symmetrized two-electron wave function in Eq.(44), R_0 is the wave functions of a single hole in Eq.(2), and R_e^0 is the wave function of a single resident electron in Eq.(17).

Figures 5e and 5f show the dependence of the overlap integral squared, K_{tr^-} , for the negatively charged trion on the CdSe core radius, a , and the CBO, $|U_{\text{Off}}|$. One can see from these figures that K_{tr^-} always increases with a and $|U_{\text{Off}}|$. At the same time the figures show that for each a there is critical $|U_{\text{Off}}|$ and vice versa where K_{tr^-} vanishes. These critical points are connected with the delocalization of the resident electron into the CdS shell. As we show above, the delocalization condition is described as $w_0^{cr} = a\sqrt{2m_{\text{CdSe}}|U_{\text{Off}}|/\hbar} \approx 1.296$. At this condition the spread of the electron wave function into the CdS shell vanishes the overlap integral.

Taking a sum over all light polarizations in Eq.(61), we obtain the radiative decay rate from the negative trion ground state as

$$\frac{1}{\tau_{3/2}^{tr^-}} = \frac{K_{tr^-}}{2\tau_0}. \quad (63)$$

As in the case of the positively charged trion, the radiative decay time of the negatively charged trion is different from the radiative decay time of the first optically active exciton only by the overlap integral. For the negative trion excited states with $M = \pm 1/2$, we have following transition probabilities:

$$T(-1/2, -1/2; \pi) = T(1/2, 1/2; \pi) = \frac{2K_{tr^-}P^2}{3} \cos^2 \theta, \quad (64)$$

$$T(1/2, -1/2; \pi) = T(-1/2, 1/2; \pi) = \frac{K_{tr^-}P^2}{6} \sin^2 \theta, \quad (65)$$

Taking a sum of the transition probabilities over all states and light polarizations, we obtain the radiative decay rate of the negative trion with $M = \pm 1/2$:

$$\frac{1}{\tau_{1/2}^{tr^-}} = \frac{K_{tr^-}}{2\tau_0}. \quad (66)$$

The radiative decay time of the trion excited state, $\tau_{1/2}^{tr^-}$, is the same as one for the ground state: $\tau_{1/2}^{tr^-} = \tau_{3/2}^{tr^-}$.

IX. DISCUSSION

This paper has developed a theoretical background for qualitative and quantitative analyses of multiple experimental measurements conducted in CdS/CdS core/thick shell NCs

and CdSe/CdS dots-in-rods nanostructures (NS). The major unusual properties of these NS are connected with the relatively small, and temperature and strain dependent conduction band offset, which provides only weak confinement of electrons in the CdSe core, while the large valence band offset in these NS leads to the strong confinement of holes. As a result, the Coulomb potential created by strongly confined holes plays an important role in electron confinement.

The optical properties of such NS should be considered to be in the *intermediate* confinement regime.³¹ The calculation procedure consists of several steps: (i) finding the energy spectra and wave function of strongly confined holes; (ii) calculation of the adiabatic Coulomb potential created by the hole charge distribution; and, finally, (iii) calculation the energy spectra of the electron moving into the total potential created by the conduction band offset and by the Coulomb potential. In this paper, we realized this program assuming that the thickness of CdS shell is much larger than the radius of electron localization around the CdSe core. The limit is satisfied in "giant" CdSe/CdS core/shell NCs grown by the Los Alamos^{2,4-7,9,15} and Deburter^{1,3,30} groups. The theory could be extended, however, to quantitative consideration of CdSe/CdS dots-in-rods NS and/or to take into account the finite thickness of the CdS shell.

Some effects of the finite CdS shell can be taken into account quantitatively on the basis of the current calculations if the radius of electron localization around the CdSe core, ζa , is smaller than the CdS layer thickness. For example, the negative trion ionization energy should be increased on the energy of the first confined level in CdS NCs with the same shape and size as original CdSe/CdS core/shell NCs. The radiative decay of the negative charged trion also does not vanish in NC with finite shell thickness when a delocalization condition is reached. The time can be calculated by replacing R_e^0 in Eq. (62) with the wave function of the the first confined level in CdS NCs.

In the paper we have also derived general expressions for the radiative decay time of the band-edge trions in various NCs. The calculations show that these times are proportional to $2\tau_0/K_{tr\pm}$. The major difference in these times is connected with the square of the overlap integral between electron and hole wave functions in positively charged K_{tr+} and negatively charged K_{tr-} trions. In CdSe/CdS core/thick shell NCs where the electron exchange energy becomes smaller than the temperature, the radiative decay time of excitons is two times longer than $2\tau_0/K_{ex}$ given by Eq. (49) due to the equal population of the Dark and Bright

exciton states.

A detailed comparison of our calculations with experimental data on the optical properties of the CdSe/CdS core/shell NCs requires a knowledge of the temperature dependence of the conduction band offset. This temperature dependence suggested first in Ref. 14 is not universal, because it has a strain contribution¹³ and should depend on the sample preparation technique. Nevertheless, the decrease of the radiative decay time by a factor of two observed in Refs. 9 and 30 is consistent with an increase of the overlap integral squared with the CBO increased from 100 to 300 meV. The small splitting of the Dark/Bright exciton states measured in the giant CdSe/CdS NCs¹⁵ is also in qualitative agreement with our calculations.

In summary, we have developed a theory of the optical properties of CdSe/CdS core/thick shell NCs. The calculations takes into account the complex structure of the CdSe valence band and inter-particle Coulomb and exchange interaction. The theory describes the fine structures and radiative decay time of excitons and positively and negatively charged trions. The results of our calculations are in qualitative agreement with experimental data available for these NCs. We believe that calculated energy spectra of negatively and positively-charged trions will explain suppression of nonradiative Auger processes observed in these structures.

ACKNOWLEDGMENTS

The authors thank J. Feldman for the critical reading of the manuscript. A.S. acknowledges support of the Center for Advanced Solar Photophysics (CASP) an Energy Frontier Research Center founded by OBES, OS, U.S. DOE. A.V.R. is grateful for the financial support received from the Swiss National Science Foundation. A. L. E. acknowledges support of the Office of Naval Research and Alexander-von-Humboldt Foundation.

Appendix: Normalization constant

From the normalization condition for an electron bound to the singly or doubly charged core we obtain the following analytical expression for the normalization constant squared:

$$B^2 = \frac{256 [2(\alpha^2 - 1)\zeta + \alpha^2\mu]^2}{\alpha^3 [q(\mu, \alpha, \zeta) + \sqrt{2\pi} \exp(2/\alpha^2) \operatorname{erf}(\sqrt{2}/\alpha) p(\mu, \alpha, \zeta)]}$$

where $p(\mu, \alpha, \zeta)$ and $q(\mu, \alpha, \zeta)$ are given by

$$\begin{aligned}
 q(\mu, \alpha, \zeta) &= 16\alpha\zeta^2(4 - 55\alpha^2) + 256\alpha\zeta^3(2 + 2\zeta + \zeta^2) + 16\alpha^3\zeta\mu(27\alpha^2 - 4) \\
 &\quad + 4\alpha^5\mu^2(4 - 15\alpha^2) \\
 p(\mu, \alpha, \zeta) &= 4\zeta^2(16 - 56\alpha^2 + 55\alpha^4) + 4\alpha^2\zeta\mu(40\alpha^2 - 27\alpha^4 - 16) \\
 &\quad + \alpha^4\mu^2(16 - 24\alpha^2 + 15\alpha^4)
 \end{aligned}$$

and $\text{erf}(x)$ is the error function defined as

$$\text{erf}(x) = \frac{2}{\sqrt{\pi}} \int_0^x e^{-t^2} dt$$

-
- ¹ B. Mahler, P. Spinicelli, S. Buil, X. Quélin, J.-P. Hermier, and B. Dubertret, *Nature Materials* **7**, 659 (2008).
- ² Y. Chen, J. Vela, H. Htoon, J. L. Casson, D. J. Werder, D. A. Bussian, V. I. Klimov and J. A. Hollingsworth, *J. Am. Chem. Soc.* **130**, 5026 (2008).
- ³ P. Spinicelli, S. Buil, X. Quélin, B. Mahler, B. Dubertret, and J.-P. Hermier, *Phys. Rev. Lett.* **102**, 136801 (2009).
- ⁴ C. Galland, Y. Ghosh, A. Steinbrück, M. Sykora, J. A. Hollingsworth, V. I. Klimov, and H. Htoon, *Nature* **479** 203 (2011).
- ⁵ H. Htoon, A. V. Malko, D. Bussian, J. Vela, Y. Chen, J. A. Hollingsworth, and V. I. Klimov, *Nano Letters* **10**, 2401 (2010).
- ⁶ Y.-S. Park, A. V. Malko, J. Vela, Y. Chen, Y. Ghosh, F. García-Santamaría, J. A. Hollingsworth, V. I. Klimov, and H. Htoon, *Phys. Rev. Lett.* **106**, 187401 (2011).
- ⁷ F. García-Santamaría, Y. Chen, J. Vela, R. D. Schaller, J. A. Hollingsworth, and V. I. Klimov, *Nano Letters* **9**, 3482 (2009).
- ⁸ Al. L. Efros, *Nature Materials* **7**, 612 (2008).
- ⁹ C. Galland, Y. Ghosh, A. Steinbrück, J. A. Hollingsworth, H. Htoon, and V. I. Klimov, *Nature Comm.* **3**, 908 (2012).
- ¹⁰ F. García-Santamaría, S. Brovelli, R. Viswanatha, J. A. Hollingsworth, H. Htoon, S. A. Crooker, and V. I. Klimov, *Nano Letters* **11**, 687 (2011).
- ¹¹ X. Y. Wang, X. F. Ren, K. Kahen, M. A. Hahn, M. Rajeswaran, S. Maccagnano-Zacher, J. Silcox, G. E. Cragg, Al. L. Efros, and T. D. Krauss, *Nature* **459**, 686 (2009).

- ¹² G. E. Cragg and Al. L. Efros, *Nano Lett.* **10**, 3131 (2010).
- ¹³ V. Dzhagan, B. Dubertret, E. Cassette, C. Javaux, R. D. Rodriguez, and D. R.T. Zahn, to be published.
- ¹⁴ G. Rainò, T. Stöferle, I. Moreels, R. Gomes, J. S. Kamal, Z. Hens, and R. F. Mahrt, *ACS Nano* **5**, 4031 (2011).
- ¹⁵ S. Brovelli, R. D. schaller, S. A. Crooker, F. García-Santamaría, Y. Chen, R. Viswanatha, J. A. Hollingsworth, H. Htoon, and V.I. Klimov, *Nature Comm.* **2**, 280 (2011).
- ¹⁶ The Landolt Börnstein Database, Springer.
- ¹⁷ A. I. Ekimov, F. Hache, M. C. Schanne-Klein, D. Ricard, C. Flytzanis, I. A. Kudryavtsev, T. V. Yazeva, A. V. Rodina, and Al. L. Efros, *J. Opt. Soc. Am. B* **10**, 100 (1993)
- ¹⁸ B. L. Gel'mont and M. I. D'yakonov, *Sov. Phys. Semiconduct.* **5**, 2191 (1973).
- ¹⁹ A. R. Edmonds, *Angular Momentum in Quantum Mechanics* Princeton University Press, Princeton, New Jersey, 1957.
- ²⁰ G. L. Bir and G. E. Pikus, *Symmetry and Strain-Induced Effects in Semiconductors* (Wiley, New York 1975).
- ²¹ Al. L. Efros, *Phys. Rev. B* **46**, 7448 (1992).
- ²² Al. L. Efros, M. Rosen, M. Kuno, M. Nirmal, D. J. Norris, and M. Bawendi, *Phys. Rev. B* **54**, 4843 (1996).
- ²³ Al. L. Efros and A. V. Rodina, *Phys. Rev. B* **47**, 10005 (1993).
- ²⁴ A.V. Rodina and Al. L. Efros, *Phys. Rev. B* **82**, 125324 (2010).
- ²⁵ Al. L. Efros and A. V. Rodina, *Solid State Commun.* **72**, 645 (1989).
- ²⁶ *Handbook of Mathematical Functions*, eds. M.Abramowitz and I. A. Stegun, National Bureau of Standards, 1998.
- ²⁷ L. D. Landau and E. M. Lifshitz, *Quantum Mechanics (Non-Relativistic Theory)* Pergamon Press, Oxford, 1977.
- ²⁸ Al. L. Efros, "Fine structure and polarization properties of the band edge excitons in semiconductor nanocrystals," Ch. 3 in the book "Semiconductor and Metal Nanocrystals: Synthesis, Electronic and Optical Properties," Ed. V. Klimov, Pergamon Press (2003).
- ²⁹ H. A. Bethe and E. E. Salpeter, *Quantum Mechanics of one- and two- electron atoms*, Springer-Verlag, Berlin-Göttingen-Heidelberg, (1957).
- ³⁰ C. Javaux, B. Mahler, B. Dubertret, A. Shabaev, A. V. Rodina, Al. L. Efros, D. R. Yakovlev,

F. Liu, M. Bayer, G. Camps, L. Biadala, S. Buil, X. Quélin, and J.-P. Hermier, to be published.

³¹ Al. L. Efros and A. L. Efros, *Sov. Phys. Semicond.* **16**, 772 (1982).